PHYSICAL REVIEW B **76**, 075119 (2007)

Calculation of temperature dependence of electrical resistivity in the transuranium metals and their alloys

Yu. Yu. Tsiovkin,* M. A. Korotin, A. O. Shorikov, and V. I. Anisimov
Institute of Metal Physics, Ural Division of Russian Academy of Sciences, S. Kovalevskaya street 18, 620041 Ekaterinburg, Russia

A. N. Voloshinskii
Moscow State Institute of Radio Engineering, Electronics, and Automation, Vernadsky av. 78, 119454 Moscow, Russia

A. V. Lukoyanov, E. S. Koneva, A. A. Povzner, and M. A. Surin
Ural State Technical University-UPI, Mira street 19, 620002 Ekaterinburg, Russia

(Received 18 May 2007; revised manuscript received 10 July 2007; published 16 August 2007)

The temperature dependence of electrical resistivity (ER) in fcc transuranium metals—plutonium, americium, and curium and some plutonium-based dilute alloys—has been considered within the Mott two-band conductivity model. It has been shown that the physical origin of the experimentally obtained temperature dependence of ER, including negative temperature coefficient of resistivity (TCR), is an ordinary electron-phonon interaction and its interference with electron-impurity interaction in the case of dilute alloys. A simple criterion of the negative TCR at high temperatures ($T > \theta_D$) was formulated and applied to explain qualitatively the experimental TCR data in Pu-based dilute alloys. To make numerical evaluation of ER of pure metals and their alloys at high temperature, the coherent potential approach for the Mott two-band conductivity model was combined with *ab initio* obtained fcc Pu, Am, and Cm densities of states as the starting point in the iteration procedure. The fcc curium LDA+U+SO density of states was reported and discussed in detail. The results of the ER theoretical investigations were compared with available experimental data.

DOI: 10.1103/PhysRevB.76.075119 PACS number(s): 72.10.−d, 72.15.Eb

I. INTRODUCTION

The experimental discovery[1] of anomalous electrical resistivity (ER) temperature behavior in some Pu-based dilute alloys (also often referred to as δ-Pu) more than 50 years ago attracted a great deal of attention of the physical community.[2–6] In americium, further investigations have shown unusual coexistence of typical "metallic" ER temperature dependence at high temperature ($T > \theta_D$, where θ_D is a Debye temperature) and $\rho \sim T^{4\pm0.5}$ regularity at low temperature ($T < \theta_D$).[7,8] On the other hand, the ER of curium resembles that of ordinary antiferromagnets: it is a quasilinear function at high temperature and is proportional to T^2 at low temperature,[9] with typical anomalies in the vicinity of the Néel temperature for all antiferromagnets. Such variety of observed ER temperature dependencies of similar metals is a nonordinary fact itself.

Many empirical or semiempirical models of conductivity[10] were used in previous theoretical investigations to describe the anomalies in ER behavior in δ-Pu. Note, at first, that description of ER behavior at low and high temperatures by combining two separate models[1,11] meets serious problems due to physical inconsistency of their bases.

Some attempts to consider δ-Pu as a *pure metal* within Kondo[12,13] and spin-fluctuation[14] models have been previously undertaken. However, no visible progress was achieved within common Kondo model.[12] Another attempt of Kondo model with specific treatment of experimental data was made in Ref. 13, however, it is very problematic and highly ambiguous to distinguish the "magnetic" part of ER.[15]

At high temperatures the dynamic spin-density fluctuation model[14] predicts negative temperature coefficient of resistivity (TCR) for some particular values of the Stoner parameter. However, its value, which provides negative TCR, was found to be unreasonably high.[10,12] Moreover, according to this model, the external magnetic field has to suppress spin fluctuations and, therefore, causes an essential change in observable ER temperature dependence, which was not found in experiments.[6,10] On the other hand, this model predicts true-like behavior $\rho \sim T^2$ at low temperatures, in agreement with available δ-Pu experimental data. However, one cannot say whether this correlation is physically based or fortuitous, because other scattering channels (electron-electron, for example) can provide similar low-temperature ER behavior. The unambiguous apportionment of dominating scattering channel in such systems at low temperature becomes difficult due to uncertainty of values of correspondent matrix elements for different types of interactions.

It is a well-known fact that different types of ER curves as well as negative TCR may be successfully explained using a synthetic model of the density of states (DOS) and simple relation for ER as a product of "ideal" resistivity (due to electron-phonon or electron-paramagnon scattering) and a function of the first and second derivatives of DOS with respect to energy at the Fermi level, by varying their values.[16] In terms of this approach, to describe the anomalous ER behavior, a number of specific, maybe questionable, assumptions concerning the shape of DOS near the Fermi level sometimes were used.[10] To reach agreement with experiment, one has to assume that the Fermi level cuts the DOS curve in the kT vicinity of strong singularity point and that the values of DOS and its derivatives are rapidly changing functions of energy. On the other hand, such behavior of DOS value and its derivatives can lead to suitable corrections

©2007 The American Physical Society

for both ER temperature dependence, magnetic susceptibility, and the electron part of heat capacity, since their values are proportional to $g_f(E_F)$. Suitable measurements show that magnetic susceptibility in some δ-Pu alloys is a constant or a weakly decreasing function of temperature.[13,17,18] The measurements of the heat capacity in $\mathrm{Pu}_{0.95}\mathrm{Al}_{0.05}$ demonstrate[19] that its electron part is a weakly decreasing function of temperature at 100–300 K. Magnetic susceptibility, obtained in americium[7] and curium,[20] in paramagnetic phases, is also a weakly changing function of temperature at 100–300 K. These facts allow one to conclude that in the fcc-Pu stabilized by impurities, Cm, and Am, the Fermi level cuts the DOS curve in a point without any singularity in kT vicinity of the Fermi level, and the $g_f(E_F)$, $g_f'(E_F)$, and $g_f''(E_F)$ values change slowly with temperature. Moreover, there is no need to make any assumptions about the DOS shape near the Fermi level in model simulations, since now it is possible to calculate the DOS of the metals using *ab initio* methods.

The explanation of the anomalies in ER behavior in Pu-based alloys was found recently within an ordinary Mott conductivity model without any assumptions concerning the intensity of electron-impurity and electron-phonon interactions using *ab initio* calculated DOS of pure plutonium.[21] It seems possible that this approach can be successfully applied to consider ER behavior in other artificial metals and their alloys, with *ab initio* DOS of pure metals as a starting point of model calculations.

The DOS and other ground state properties of solid states can be determined by modern numerical calculations based on the density functional theory.[22] For example, the standard local (spin) density approximation with accounting for Hubbard (U) interaction [L(S)DA+U] allows one to reproduce well the ground state properties of many compounds except plutonium and metals beyond it in the Periodic Table.[23] The difficulty in describing the electronic structure and ground state properties of actinide metals and their compounds is due to the comparable strength of spin-orbit (SO) coupling (about 1 eV for Pu) and exchange (Hund's) interaction (about 0.5 eV).

Numerous band methods based on the density functional theory have been applied to investigate the electronic structure of plutonium. Approving a well-known fact that the density functional theory can correctly reproduce experimental crystal structures, in Ref. 24 a phase diagram of plutonium was found in good agreement with experiment. Investigations carried out in the frame of the LDA+U+SO method demonstrated that the nonmagnetic ground state of plutonium is provided by $J=0$ total moment and can easily be broken.[23] This conclusion agrees well with the result of the "around-the-mean-field" version of LDA+U.[25] The resulting DOS shows that the spin-orbit coupling leads to sufficiently separated fulfilled $j=5/2$ subband, which is located just below the Fermi level, and almost empty $j=7/2$ subband, which is shifted by strong Coulomb interaction to 3–4 eV above the Fermi level. This result is determined by the f^6 configuration of the plutonium f shell. Recent experiments revealed f^5 configuration in δ plutonium.[26] Better agreement with experiment can be found in other calculations.[24,27] Other references could be found elsewhere.[23,28]

The LDA+U+SO method predicts the nonmagnetic ground state of pure Pu metal or antiferromagnetic ground states if any crystal structure distortions arise due to interstitial atoms or vacancies. This fact has been justified experimentally.[29] The method mentioned above predicts a reasonable, but not large, value of DOS at the Fermi level since dynamical many-body effects are not taken into account. This disagreement with high values of heat capacity could also be explained if more accurate analysis of experimental data is performed. One should take into account that the heat capacity was measured for $\mathrm{Pu}_{0.95}\mathrm{Al}_{0.05}$ alloy, and extracting the electronic part of heat capacity from this experiment to describe the values and features of DOSs of *pure* Pu looks very problematic. Moreover, the DOS value at the Fermi level, extracted from the magnetic susceptibility data, is not large and agrees better with the one calculated within around-the-mean-field version of LDA+U and LDA+U+SO approaches.[23,25,28]

The dynamical mean-field theory (DMFT) should be applied in order to reproduce experimental photoemission spectra.[30,31] The simple application of this method with interpolation formula[31] resulted in a large value of the DOS at the Fermi level, in agreement with experimentally observed photoemission spectra and heat capacity measurements,[19] but gave an incorrect ferromagnetic ground state. Summarized modern experimental data of magnetic properties of Pu metal finally proved that pure plutonium metal in δ and α phases and some of its alloys are nonmagnetic[32] or have a magnetic moment less than $10^{-3}\mu_B$ at 4 K.[29,33]

Further DMFT calculations with numerically exact impurity solvers are difficult at the moment. So some simplifications for plutonium, americium, and curium ground state investigation were used,[34–36] including the perturbative T-matrix and FLEX method in Ref. 37 and vertex corrected one-crossing approximation in Ref. 34. Some works concentrated on the Hubbard-I approximation only.[35,36] This allows one to reproduce equation of state for americium and some features of a photoemission spectrum, but is still far from completeness.

We have chosen the LDA+U+SO DOSs of actinides under consideration as a starting point for coherent potential approximation (CPA) simulations. Note that calculation results are in good agreement with available data on magnetic moment and spectral properties.

Based on the obtained electron ground state, one can conclude that plutonium, americium, and curium are ordinary members of the transition metal family, distinguished by strongly localized f-electron states only. It becomes quite unclear how to justify from this point of view the well-known anomalies in temperature dependencies of ER of some Pu-based dilute alloys, on the one hand, and obtained ordinary metallic type of ER behavior of curium and americium, on the other hand.

In this paper, starting from results of numerical simulations for fcc plutonium, americium,[23,28] and curium, the ER behavior of these metals and some Pu-based alloys has been analyzed from the most general point of view within single conductivity model. Thus we have avoided the necessity of some synthetic and debatable models[1,11–13] and any assumptions concerning the specificity of DOS near the Fermi level.[10,11,13,14,38] Also no assumptions concerning weakness of the interaction have been made for all of the systems under consideration. We have also accounted for renormalization effects on the electron ground state from phonon subsystem at final temperatures in ER calculations.

II. MODEL AND COHERENT POTENTIAL APPROXIMATION EQUATIONS

To analyze ER of plutonium-based alloys, we start from the Mooij empirical rule.[39] According to this rule, the negative TCR correlates with high ER values ($\sim 100-140\ \mu\Omega$ cm). Note, at first, that high ER values in the Pu-based alloys are due to very high *residual resistivity* rating above 80 $\mu\Omega$ cm.[2–4] Thus residual resistivity contribution over the temperature interval of negative TCR dominates. However, this fact has never been taken into account, but, in our opinion, its proper accounting is rather important.

Second, the negative TCR in Pu-based dilute alloys was observed only either for very *light* (Al, Si, Ga, and others) or very *heavy* (Np, Am, and Cm) impurities. Such specific sensitivity to impurity mass gives evidence that the effect of ion mass defect, i.e., electron-phonon interaction, may be a clue point not only in understanding the problem of plutonium crystal lattice stability under doping[40] but also in understanding the anomalous ER behavior. The fact that the negative TCR emerges only near and above the Debye temperature (~ 100 K) gives an additional argument in favor of this point of view.

Let us consider the systems of s, d, and f electrons within Mott conductivity model,[41] performing intra- and interband transitions as a result of their scattering at randomly distributed Coulomb fields of impurity ions at finite temperature. The Hamiltonian of the electron subsystem can be written in the following form:[42]

$$\hat{H}=\sum_{l} E_l a_l^{\dagger} a_l + \frac{1}{N}\sum_{n,l,l'} e^{-i(\vec{k}-\vec{k}',\vec{R}_n)}\hat{B}_{ll'}(n) a_l^{\dagger} a_{l'}, \qquad (1)$$

where E_l is a periodical part of electrons energy. Combined index l includes the band index j ($j=s,d,f$) and wave vector $\vec{k}$; $\vec{R}_n$ is a radius vector of the nth site of a crystal lattice.

$$\hat{B}_{ll'}(n)=\nu(n)\Delta V_{ll'}+\sum_{\alpha} a_{\alpha}(n)\hat{Q}_{\alpha,l,l'}(n), \qquad (2)$$

where $\Delta V_{ll'}=V^{A}_{ll'}-V^{B}_{ll'}$ describes the intensity of the electron-impurity part of the interaction, whereas the periodical part of this interaction is included in E_l. The $\nu(n)=\alpha_B(n)c_A-\alpha_A(n)c_B$ factor randomly distributes ions of alloy components along the sites of a crystal lattice. $\alpha_{A(B)}(n)=1$ if the nth site is occupied by an ion of the $A(B)$ type, and $\alpha_{A(B)}(n)$ equals zero in the opposite case. Here, c_A and c_B are alloy component concentrations. Operator $\hat{Q}_{\alpha,l,l'}(n)$ describes the intensity of electron-phonon interaction. If thermal displacements of ions are small, the operator $\hat{Q}_{\alpha,l,l'}(n)$ can be written as

$$\hat{Q}_{\alpha,l,l'}(n)=Z_{\alpha,ll'}\frac{-i}{\sqrt{N}}\sum_{\vec{q}}\sqrt{\frac{q_0}{q}}\left[e^{i(\vec{q}\vec{R}_n)}\hat{b}_{\vec{q}}-e^{-i(\vec{q}\vec{R}_n)}\hat{b}^{\dagger}_{\vec{q}}\right], \qquad (3)$$

where

$$Z_{\alpha,ll'}=\left(\frac{\hbar K_F}{2M_{\alpha}S_{\alpha}}\right)^{1/2}\left(\frac{2K_F}{3q_0}\right)^{1/2}C_{\alpha,l,l'} \qquad (4)$$

are the constants of intensity of intra- and interband transitions due to electron-phonon scattering. M_{α} is the α-ion mass, S_{α} is the sound velocity in α-type metal, q_0 is the maximum value of q, K_F is the Fermi wave number of electron, and $C_{\alpha,l,l'}$ is a (Bloch) constant of electron-phonon coupling.

The elements of electron-phonon interaction matrix include two parts—dependent on and independent of ion stochastic distribution. Namely, the splitting of electron-phonon coupling into two parts allows one to understand the physical meaning of the effect of impurity mass defect.

The s, p, d, and f bands overlap and, therefore, hybridization effects have to be taken into account. However, it is well known that these effects lead only to renormalization of the electron ground state Hamiltonian and do not change its scattering part, therefore it will be assumed that these effects are accounted for in the electron ground state. For the sake of simplicity, we keep the same band names after renormalization.

As has been pointed out above, the electron-impurity interaction is not weak. Therefore, contributions from different types of scattering to total ER may not be summed up in a simple additive way, since the interference between them is not negligible *a priori*. That is why one has to use calculation methods, the validity of which is not limited by the interaction intensity and they enable one to account for the complex structure of d-, f-DOS and its deformation due to electron-impurity and electron-phonon interactions.

Let us determine the total resolvent of the full energy operator $\hat{H}$:

$$\hat{R}=(z-\hat{H})^{-1} \qquad (5)$$

and the strictly diagonal part of the total resolvent $\hat{R}$ in the $\hat{H}_0$ representation:

$$\hat{G}=(z-\hat{H}_0-\hat{\Delta})^{-1}, \qquad (6)$$

where $\hat{\Delta}$ is a strictly diagonal shift operator in the $\hat{H}_0$ representation. Broadening of single electron levels is described as

$$\hat{\Delta}=\frac{1}{N}\sum_{n,l,l'} e^{-i(\vec{k}-\vec{k}',\vec{R}_n)}\Delta_j\delta_{jj'}a_l^{\dagger}a_l. \qquad (7)$$

The real part of the coherent potential Δ_j determines the shift η_j, and its imaginary part γ_j determines the broadening of single-electron levels.

To derive equations within two-band CPA, the Dawson identity was used:

$$\hat{R}=\hat{G}+\hat{G}(\hat{V}-\hat{\Delta})\hat{R}. \qquad (8)$$

Scattering operator $\hat{T}$ can be determined in a convenient form as

$$\hat{R}-\hat{G}=\hat{G}\hat{T}\hat{G}. \tag{9}$$

Multiplying both right and left parts of identity (9) by $\hat{G}^{-1}$, the following expression for the scattering operator is obtained:

$$\hat{T}=\hat{G}^{-1}(\hat{R}-\hat{G})\hat{G}^{-1}. \tag{10}$$

This expression allows further to determine the order of matrix products uniquely and avoid difficulties associated with the choice of right- or left-matrix products. Using the Dawson identity (8) and expression (10) for the shift operator, one obtains the following operator series:

$$\hat{\Delta}=[(\hat{V}-\hat{\Delta})\hat{G}(\hat{V}-\hat{\Delta})+(\hat{V}-\hat{\Delta})\hat{G}(\hat{V}-\hat{\Delta})\hat{G}(\hat{V}-\hat{\Delta})+\cdots]_{diag}. \tag{11}$$

The *diag* index means that the diagonal part in the $\hat{H}_0$ representation of the sum of operator products in brackets should be taken. It was shown in Ref. 46 that the series (11) contains mutually compensated block terms, in which the shift operator is included in indirect form. Excluding the compensated block terms from Eq. (11), one finally obtains the shift operator as

$$\hat{\Delta}=[\hat{V}\hat{G}\hat{V}+\hat{V}\hat{G}\hat{V}\hat{G}\hat{V}+\cdots]_{D}. \tag{12}$$

The D index means that in $[\ldots]_D$ only strictly diagonal terms in the $\hat{H}_0$ representation are kept and items containing the blocks are omitted.

Summation (12) can be conveniently performed in a matrix form. Since the $\hat{G}$ and $\hat{\Delta}$ operators are strictly diagonal in the $\hat{H}_0$ representation, the Green functions, the coherent potential, and the interaction V can be determined as matrices by the band index:

$$F=\begin{bmatrix} F_s & 0 \\ 0 & F_f \end{bmatrix}, \quad \Delta=\begin{bmatrix} \Delta_s & 0 \\ 0 & \Delta_f \end{bmatrix},$$

$$V=\begin{bmatrix} B_{n,ss}(u) & B_{n,sf}(u) \\ B_{n,fs}(u) & B_{n,ff}(u) \end{bmatrix}, \tag{13}$$

where

$$F_j=\frac{1}{N}\sum_{\vec{k}}\frac{1}{(z-E_{\vec{k},j}-\Delta_j)} \tag{14}$$

is the j-band electron Green function. The $B_{n,jj'}(u)=\nu(n)\Delta V_{jj'}+Q_{jj'}(u)$ now become values independent of $\vec{k}$ and $\vec{k}'$ wave vectors. The latter are functions of fluctuating variable u. That is why the phonon operators may be replaced with the functions of fluctuating variable at high temperature.[47]

Within single-electron and single-site approaches and using notations (13) and (14), the series (12) are summed up accurately in the convergence range $|F_jB_j|<1$. For the sake of simplicity, notation $B_{n,jj}(u)=B_{n,j}(u)$ was used below. By assuming $B_{n,jj'}(u)=B_{n,j'j}(u)=B(n,u)$ for averaging ion thermal displacements, one obtains for s-band coherent potential:

$$\langle\Delta_s\rangle_{ph}=\frac{1}{N}\sum_n\int_{-\infty}^{+\infty}duP_n(u) \times\frac{B_{n,s}^2(u)F_s[1-F_fB_{n,f}(u)]+[1+F_sB_{n,s}(u)]B_n^2(u)F_f}{[1-F_sB_{n,s}(u)][1-F_fB_{n,f}(u)]-B_n^2(u)F_sF_f}, \tag{15}$$

where

$$P_n(u)=\frac{1}{\sqrt{2\pi\beta_n}}e^{-u^2/2\beta_n}$$

is the Gauss distribution function, with $\beta_n=Z_{\alpha,jj'}6T/\Theta_n$,[42,47] and θ is the Debye temperature. Full equations for Δ_s may be found from Eq. (15), after configuration averaging, i.e., summation over sites $n\in A$ and $n\in B$. The equation for coherent potential of f-band electrons is the same as Eq. (15), with the only replacement of band indices $s\rightleftarrows f$.

Neglecting interband transitions, i.e., assuming $B=0$, then, as follows from Eq. (15), two independent equations corresponding to the single-band model of CPA can be obtained:

$$\langle\Delta_f\rangle=\int_{-\infty}^{+\infty}du\left[c_AP_A(u)\frac{[c_B\Delta V+Q_{A,f}(u)]^2F_f}{1-F_f[c_B\Delta V+Q_{A,f}(u)]}+c_BP_B(u)\frac{[c_A\Delta V-Q_{B,f}(u)]^2F_f}{1+F_f[c_A\Delta V-Q_{B,f}(u)]}\right]. \tag{16}$$

The second equation may be derived from Eq. (16) by replacement of band indices $f\to s$.

Note that Eq. (16), for coherent potentials, essentially differs from the main equation in Ref. 47, since the latter was obtained assuming that the single-site scattering T-matrix averaged over both configuration and thermal displacements of ions is zero ($\ll T_n>_{ph}>_c=0$).

It is well known from the band structure *ab initio* calculations that DOS values at the Fermi energy for d and f electrons in actinides are significantly higher than those for s (p) electrons. Therefore, it is reasonable to assume $|B_{n,s}F_s|\ll 1$, $|B_nF_s|\ll 1$ and $|B_{n,s}F_s|/|B_{n,f}F_f|\ll 1$, $|B_nF_s|/|B_nF_f|\ll 1$. Then the system of Eq. (15) can be simplified, since the f-electron coherent potential equation coincides with Eq. (16) and the expression for the s-electron coherent potential is the following:

$$\langle\Delta_s\rangle=\int_{-\infty}^{+\infty}du\left[c_AP_A(u)\frac{[c_B\Delta V+Q_A(u)]^2F_f}{1-F_f[c_B\Delta V+Q_A(u)]}+c_BP_B(u)\frac{[c_A\Delta V-Q_B(u)]^2F_f}{1+F_f[c_A\Delta V-Q_B(u)]}\right]. \tag{17}$$

Equations (15)–(17) include several parameters of the theory. Parameters $\Delta V_{jj'}$ are equal to the difference in positions of the gravity centers in total energy scale in the alloy component bands. Usually within CPA they are approximated as $\Delta V_{jj'}\approx\Delta V$, and the latter can be estimated from the data of *ab initio* calculations or experimental data. Other parameters $[Z_{\alpha,jj'}$ in Eqs. (15)–(17)] can be estimated based on available experimental data.

Using the above assumptions and setting $\Delta V_{jj'}=0$ in Eq. (17), one can obtain coherent potential equations in the case of pure metal:

$$\langle \Delta_f \rangle = \int du P(u) \frac{Q_f^2(u) F_f}{1 - Q_f(u) F_f},$$

$$\langle \Delta_s \rangle = \int du P(u) \frac{Q^2(u) F_f}{1 - Q(u) F_f}. \qquad (18)$$

Note that in this limit, parameter $\beta = 2T/\Theta$.

To take into account the effect of individual electronic DOS of the alloy components on the calculations of the alloy kinetic properties in a reliable way, the CPA equations have to be solved numerically using realistic *ab initio* calculated DOS of the alloy components. The initial alloy DOS may be chosen according to the approach described in Sec. IV.

Model simplifications used in the derivation of Eqs. (16)–(18) are equivalent to the main Mott conductivity model assumptions, where only the $s \rightarrow (d)f$ interband electron transitions have been considered, since probabilities of the others are negligibly small. As a result of such simplifications, all numerical calculations within Mott conductivity model for metals and alloys at high temperature can be carried out in a well-known way, using Kubo formula for electrical conductivity.

III. SIMPLE CRITERION OF NEGATIVE TCR

The whole system of the CPA equations (15) is very difficult for direct analysis and solution. However, several simple estimations can help to analyze the ER temperature dependence qualitatively. For our reasoning, it is sufficient to consider only the main terms of the perturbation series at the *second* and *third* orders of interaction, which are linear with temperature. Since the ER is proportional to the imaginary part of the shift operator, from Eq. (15) one obtains

$$\begin{aligned}\frac{\rho}{\operatorname{Im} F_j(E_F)} &\sim c_A c_B \Delta V^2 + \{c_A Z_A^2(T/\theta_A) + c_B Z_B^2(T/\theta_B)\} \\ &\quad + 2c_A c_B\{2\Delta V[Z_{jA} Z_A(T/\theta_A) - Z_{jB} Z_B(T/\theta_B)] \\ &\quad + \Delta V_{sj}[Z_A^2(T/\theta_A) - Z_B^2(T/\theta_B)]\}\operatorname{Re} F_j(E_F),\end{aligned} \qquad (19)$$

where $F_j(E_F)$ is the Green function at the Fermi level. Expression (19) consists of three terms, and the first term describes only electron-impurity scattering and determines the value of residual resistivity. The second term corresponds to electrons scattered at the "pure" phonons. The term in the quadratic brackets describes the interference between electron-impurity and electron-phonon couplings. Assuming additionally that $Z_{j,\alpha} \approx Z_\alpha$ and $\Delta V_j \approx \Delta V$, the following simple criterion for negative TCR observability at high temperatures, i.e., $T > \theta$, can be found:

$$1 + 6 c_A c_B \Delta V \frac{Z_A^2/\theta_A - Z_B^2/\theta_B}{c_A Z_A^2/\theta_A + c_B Z_B^2/\theta_B} \operatorname{Re} F_f(E_F) \leqslant 0. \qquad (20)$$

Thus the values of ΔV, the difference between electron-phonon coupling constants of solvent and impurity, and the real part of the Green function at the Fermi level, which are available from experimental data and *ab initio* calculations, determine the TCR sign.

IV. DENSITY OF STATES OF ALLOYS USED IN COHERENT POTENTIAL APPROXIMATION

To account in a reliable way the effect of individual electronic features of the alloy components on the alloy kinetic properties, CPA equations have to be solved numerically using *ab initio* calculated DOS of alloy components. Let us assume that the number of occupied states n in each band of an alloy is equal to the average weighted number of occupied states of components:

$$n_j = \sum_{\alpha=A,B} c_\alpha n_{\alpha,j}. \qquad (21)$$

As the maximum number of f, d, and s electrons in each subband is strictly limited due to normalization of DOS, an analogous expression can be written for unoccupied states:

$$\bar{n}_j = \sum_{\alpha=A,B} c_\alpha \bar{n}_{\alpha,j}. \qquad (22)$$

Since the number of electrons in a band is defined by DOS function of components $g^\alpha(E)$, the following expressions for occupied and unoccupied states can be written respectively:

$$\int_{E_0}^{E_F} g_j(E) dE = \sum_{\alpha=A,B} c_\alpha \int_{E_{\alpha,0}}^{E_{F,\alpha}} g_{\alpha,j}(E) dE,$$

$$\int_{E_F}^{E_c} g_j(E) dE = \sum_{\alpha=A,B} c_\alpha \int_{E_{F,\alpha}}^{E_{\alpha,c}} g_{\alpha,j}(E) dE, \qquad (23)$$

where E_F and $E_{F,\alpha}$ are the Fermi energies of an alloy and its components, respectively, $E_{\alpha,0}$ are the energies of the zone bottom of the alloy and its components, and E_c and $E_{\alpha,c}$ are the alloy and its component energies, at which DOS becomes negligible. The Fermi energy can be determined by requiring DOS continuity at point E_F.

Solving Eqs. (23), one obtains expressions for the alloy DOS

$$\begin{aligned} g(E) = \sum_\alpha c_\alpha \frac{E_{F,\alpha} - E_{\alpha,0}}{E_F - E_0} g_\alpha \bigg[&\frac{E_{F,\alpha} - E_{\alpha,0}}{E_F - E_0}(E - E_0) \\ &+ E_{\alpha,0} \bigg] \quad \text{for } E \leqslant E_F \end{aligned}$$

and

$$\begin{aligned} g(E) = \sum_\alpha c_\alpha \frac{E_{\alpha,c} - E_F}{E_c - E_{F,\alpha}} g_\alpha \bigg[&\frac{E_{\alpha,c} - E_{F,\alpha}}{E_c - E_F}(E - E_F) \\ &+ E_{F,\alpha} \bigg] \quad \text{for } E \geqslant E_F. \end{aligned} \qquad (24)$$

From the same requirement (DOS continuity), the following equation can be deduced:

$$\sum_{\alpha} c_{\alpha} \frac{E_{F,\alpha} - E_{\alpha,0}}{E_F - E_0} g_{\alpha}(E_{F,\alpha}) = \sum_{\alpha} c_{\alpha} \frac{E_{\alpha,c} - E_F}{E_c - E_F} g_{\alpha}(E_{F,\alpha}), \tag{25}$$

the solution of which gives the Fermi energy of the alloy:

$$\frac{E_F - E_0}{E_c - E_F} = \frac{\sum_{\alpha} c_{\alpha}(E_{F,\alpha} - E_{\alpha,0}) g_{\alpha}(E_{F,\alpha})}{\sum_{\alpha} c_{\alpha}(E_{\alpha,c} - E_{F,\alpha}) g_{\alpha}(E_{F,\alpha})}. \tag{26}$$

To calculate alloy DOS, Eqs. (24)–(26) were solved numerically using DOS of pure components, obtained within the framework of LDA+U+SO. Using the Leman representation

$$F(z) = \int_{-\infty}^{+\infty} \frac{g(E)dE}{z - E} \tag{27}$$

the initial Green function of the alloy was found as the starting point for CPA equation numerical solution.

V. RESULTS AND DISCUSSION

A. Pu, Am, and Cm density of states

LDA+U+SO method combines the local density approximation (LDA) with additional accounting for strong on-site Coulomb interaction (U) and spin-orbit coupling (SO) written in the full matrix form. First suggested in Ref. 23, it was broadly applied to many d- and f-metal compounds. The specific benefit of this method is that it allows one to work in any coupling scheme. For 3d and 4f metals, weak SO coupling can be considered in the Russel-Sounders (LS) coupling scheme with "well-defined" **L** and **S** operators. The competition between spin-orbit and exchange (Hund) interactions of comparable strength for 5f elements leads to the more complicated picture. Both LS and jj schemes (in the latter, only total moment operator **J** is well defined) are no longer valid and an intermediate coupling scheme is needed to describe 5f shell in actinides. In order to take into account comparable SO and exchange interactions correctly, the rotation invariant form of the Hamiltonian was applied in the LDA+U+SO method. For more details of this method, see Ref. 23.

In the present investigation, high-temperature fcc phases of Pu, Am, and Cm were considered. Plutonium in the fcc phase, also known as δ-Pu, is stable from 594 to 725 K and has a lattice constant a=4.637 Å. Above 925 K or at 6.1(2) GPa, Am metal undergoes the transition into a fcc phase with[43] a=4.613 Å. At high temperature or high pressure about 17(2) GPa, Cm metal also transforms into a fcc phase.[44] In the present calculation of curium metal, the value a=4.472 93 Å was used. We set the same Coulomb U value equal to 2.5 eV for all three metals, which gives correct equilibrium volume for δ-Pu.[23] The Hund exchange parameters were calculated using "constrained LDA" procedure[45] and were found to be 0.48 eV for Pu and Am, and 0.52 eV for Cm. The Kramers-Kronig transformation was used to find the value of the real part of the total Green function at the Fermi level, which resulted in +2.3 eV^{-1} for plutonium and −2.6 and −0.8 eV^{-1} for americium and curium, respectively.

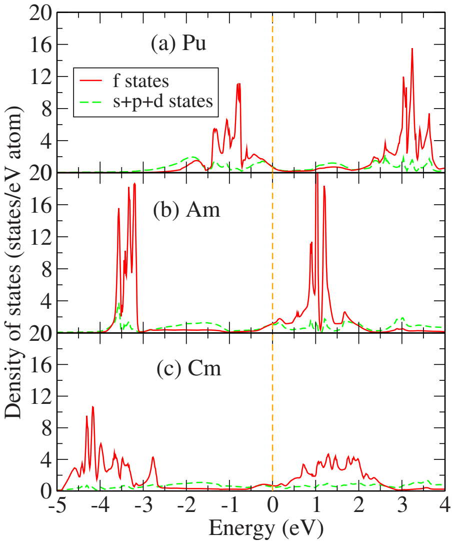

FIG. 1. (Color online) The calculated DOS of Pu, Am, and Cm using the LDA+U+SO method.

The DOS curves obtained from the LDA+U+SO calculations for all three metals are shown in Fig. 1. Those for plutonium and americium were discussed previously[23,28] in detail. The LDA+U+SO results for curium are presented in this paper. Note that although both Pu and Am could be described well in the frame of jj-coupling scheme and are found to have the same f^6 configuration with zero total moment, the obtained DOS differs drastically. For both Pu and Am, j=5/2 subband is fulfilled and j=7/2 subband is almost empty. However, whereas the Fermi level cuts the top of the fulfilled j=5/2 subband in the case of Pu, in the Am case it cuts the bottom of the empty j=7/2 subband. The center of gravity of the j=5/2 subband is positioned near 1 and 3.5 eV below the Fermi energy in Pu and Am, respectively. Curium has f^7 configuration and effective magnetic moment about 7μ_B, which lies within the range of available magnetic moment values from experiment.[48] In curium, a filled subband lies below the Fermi level from −5 to −2.5 eV and a broad empty subband is positioned just above the Fermi level up to 3 eV [see Fig. 1(c)]. In contrast to Pu and Am, where the jj-coupling scheme is valid and the occupied bands (j=5/2) contain six f electrons, in Cm some intermediate coupling scheme close to LS type takes place.[34] As a consequence of this, 7f electrons of Cm are located in an occupied subband, presenting a mixture of bands with different orbital characters. Thus the occupied subbands of Am and Cm seem similar, but their orbital character is substantially varied. The employment of the DMFT method with an approximate impurity solver[34] does not lead to drastic changes in the occupied part of the DOS, even near the Fermi level, but broadens the unoccupied part up to 5 eV.

B. Temperature coefficient of resistivity: The qualitative results

It is reasonable to suppose that in the *dilute* alloys (c_B $\leqslant$5 at. %) the solvent band structure and elastic properties

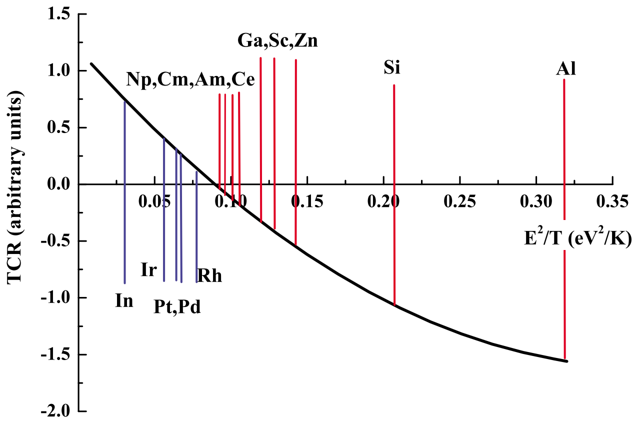

FIG. 2. (Color online) The relation between the electron-phonon coupling constant and TCR sign in dilute Pu-based alloys. The value of electron-phonon coupling constant for different types of impurity in Pu is at the intersection of vertical lines and *x* axis. For Ce, Np, Am, and Cm calculations, parameter of electron-impurity interaction value of 5 eV was used.

are almost the same as in pure metal and, for the qualitative estimations, one can assume $\theta_B \approx \theta_A$ and $S_B \approx S_A$. In this case, only the distinction between solvent and impurity ion masses determines the difference between the constants of electron-phonon interaction of metals.

Three parameters should also be determined to proceed with the calculations within the developed approach. The first parameter ΔV can be evaluated, according to Harrison,[49] as $\sim$5–8 eV. The numerical value of $\mathrm{Re}\,F(E_F)$ for these metals was determined from the *ab initio* DOS calculations. Accounting for simple Bloch estimation $C_{s-(d)f,\alpha} \sim 2/3E_{F,\alpha}$, the difference between electron-phonon constants of solvent and impurity can be evaluated.

Using experimental data on Debye temperature, sound velocity,[50] and lattice parameter in fcc Pu and applying criterion (20), one obtains the theoretical predictions on TCR in Pu-based alloys, doped with 5 at. % of various impurities, which are presented in Fig. 2.

The TCR sign in Pu-based alloys is negative in the case of doping with light impurities—Al, Ga, Ge, Si, and Sc—and positive in the case of intermediate impurity masses—Ir, Rh, Pd, Pt, and In. Almost all predictions agree with the available experimental data. Therefore, it seems possible that the observed dependence of TCR sign on impurity mass originates actually from the interference between electron-impurity and electron-phonon interactions. Note that the negative TCR is predicted for plutonium doped with very heavy impurities—Np, Am, and Cm—due to the small difference between their masses and the parameter of electron-impurity interaction value of about 5 eV. Similar behavior was found experimentally in some concentrated Pu-Am and quasidilute (8% of Am) alloys.[8] In this case, doping the host of Pu by Am impurity results in negative or zero TCR at 100–300 K due to the small difference in the masses of metals. Abandoning simplifications of equality of Debye temperatures and sound velocities for host metal and impurity, one can obtain the number of new impurities also providing negative TCR, e.g., Ce and others.

Our calculations predict "normal" metallic type of ER behavior in the case of americium- and curium-based dilute alloys due to the positive sign of the real part of the Green functions of those metals at the Fermi level. The negative sign of the real part of the Green function breaks the negative TCR condition (note that the real part of the Green function is positive in the case of Pu). However, the normal type of ER temperature dependence behavior can be disturbed in some Am- and Cm-based *concentrated* alloys if the second compound reduces the DOS of the alloy such that the real part of the Green function becomes positive.

C. Electrical resistivity of alloys: Numerical results

For ER calculations, Eq. (17) has been solved numerically by an iteration procedure using the DOS of alloy obtained according to Eqs. (24)–(26). Calculations of the electrical resistivity were carried out in relative units using Kubo formula adjusted for the CPA case,[42,51]

$$(\rho_j)^{-1} = \frac{4e^2\hbar n_j}{3\pi^2 m}\int dU\left(-\frac{df}{dU}\right) \times \int dE\, g_j(E)E\left\{\frac{\gamma_j(U)}{[U-E-\eta_j(U)]^2+[\gamma_j(U)]^2}\right\}^2 . \tag{28}$$

The matrix element of the squared electron speed in Eq. (28) is replaced by the averaged kinetic electron energy: ($\vartheta_x^2 \approx 2\bar{E}/m$). However, this rather rough approximation has no effect on the final result, since the ER behavior obtained with different values of this matrix element is almost the same. Apparent restriction on the validity of Eq. (28) exists due to neglecting reverse $f(d) \rightarrow s$ transitions of conductivity electrons. This neglect is suitable only in the case where the ratio between DOSs of f (d) and s bands is large. Note that all results of ER calculations were obtained in arbitrary units. All results of numerical calculations of ER temperature dependences of $\mathrm{Pu_{0.95}Ga_{0.05}}$ and $\mathrm{Pu_{0.95}Al_{0.05}}$ alloys, presented in this section, were obtained using the experimental data for theory parameters (sound velocities and Debye temperatures) of alloy compounds without any simplification mentioned above in Sec. V B.

The comparison of ER in Pu stabilized with 5 at. % Al and Ga, calculated within Kubo formula, with available experimental data is shown in Fig. 3. One can see that the theoretical curves for Pu-based alloys fit well the experimental data. Negative TCR was calculated in $\mathrm{Pu_{0.95}Ga_{0.05}}$ alloys at 100–300 K, and at 100–350 K temperature range in the case of $\mathrm{Pu_{0.95}Al_{0.05}}$ alloy. Numerical results agree well with available experimental data and correlate qualitatively with TCR criterion Eq. (20).

One can see from Fig. 2 that the difference between the constant of electron-phonon coupling of host and impurity in alloy doped with Al is greater than in the case of $\mathrm{Pu_{0.95}Ga_{0.05}}$. So the negative TCR condition in $\mathrm{Pu_{0.95}Al_{0.05}}$ alloy is fulfilled at higher temperature. It was found that the TCR of $\mathrm{Pu_{0.95}Ga_{0.05}}$ alloys changes sign above 250 K and is positive up to 700 K. In the case of $\mathrm{Pu_{0.95}Al_{0.05}}$, negative TCR con-

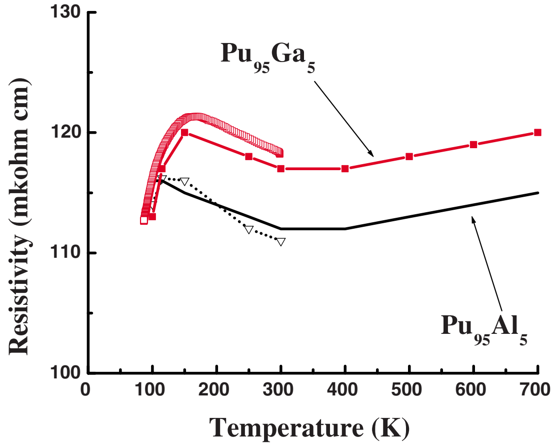

FIG. 3. (Color online) Temperature dependence of ER in $Pu_{0.95}Al_{0.05}$ and $Pu_{0.95}Ga_{0.05}$: experimental (Refs. 5 and 13; dashed line) and theoretical (solid line) data. For $Pu_{0.95}Ga_{0.05}$ alloys, generalized data of Ref. 52 were used.

dition is fulfilled at 350 K, and ER has normal metal behavior up to 700 K.

Obtained results for this alloys demonstrate that the electron-impurity and electron-phonon interactions significantly smooth all initial sharp singularities in the DOS curve and result in a decrease of the DOS value at the Fermi level with temperature.[21] Note that a similar result was observed experimentally by Lashley *et al.*[19] in δ-Pu doped with 5 at. % Al in the heat capacity measurements. The comparison between the DOS value at the Fermi level calculated with CPA and one extracted from the heat capacity (C_{el}/T) shows that both DOS and heat capacity are weakly increasing functions of temperature.[21] The magnetic susceptibility measurements of the same Pu-based alloys also demonstrate the drop of DOS values at the Fermi level with temperature.[13,17,18]

This good agreement between theoretical and experimental data with respect to DOS as well as ER behavior with temperature gives evidence in favor of our approach, which takes into account interference between electron-impurity and electron-phonon interactions. Our approach allows us also to avoid various assumptions of unknown reliability often used previously to describe the negative TCR as well as $\sim T^2$ dependence. The presented model provides also the comprehension of ER behavior at low temperatures. It was found in the previous works[53,54] that in dilute alloys characterized by interference between electron-impurity and electron-phonon interactions, Mott model predicts $\rho(T) \sim T^2$ regularity at low temperatures in contrast to $\rho(T) \sim T^3$, which is typical in the alloys *without* interference. Thus all the observed features of ER behavior, both at low and high temperatures, can be explained within the single model without any specific assumption of DOS structure at the Fermi level.

D. Electrical resistivity of pure metals: Numerical results

Results of our CPA calculations [Eqs. (18)] of ER in pure fcc Pu, Am, and Cm using Bloch constant value $\sim 0.8 E_F$ (Ref. 50) are shown in Fig. 4. High values of ER in these metals are a consequence of $s \rightarrow d$ and $s \rightarrow f$ transitions of scattering electrons. Weak nonlinearity in ER temperature behavior in Pu and Am above θ_D is caused by DOS erosion at the Fermi level due to electron-phonon interaction (see Fig. 5).

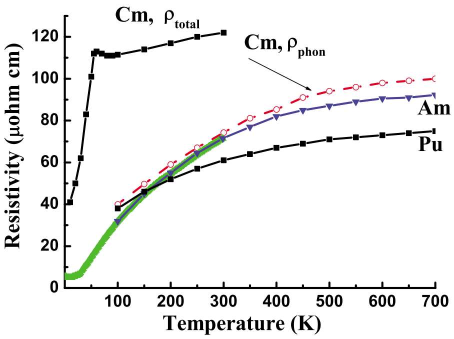

FIG. 4. (Color online) Temperature dependence of ER in Pu, Am, and Cm: experimental (Refs. 7 and 9 dashed and thick lines) and theoretical (solid line) data.

Recently, the experimental data of ER in Cm metal for the α phase only have been published. Total ER was found as the sum of residual resistivity (more than 40 $\mu\Omega$ cm), magnetic part of resistivity, and the part of ER originated from electron-phonon coupling.[9] The magnetic part of ER was found as the difference between the total resistivities of Cm and Am. Note, at first, that the large value of residual resistivity shows that used samples of metal contained essential number of impurities, including noncontrolled ones. Second, nothing can be said about the reliability of the suggestion, proposed in Ref. 9, that ER is the sum of additive values,

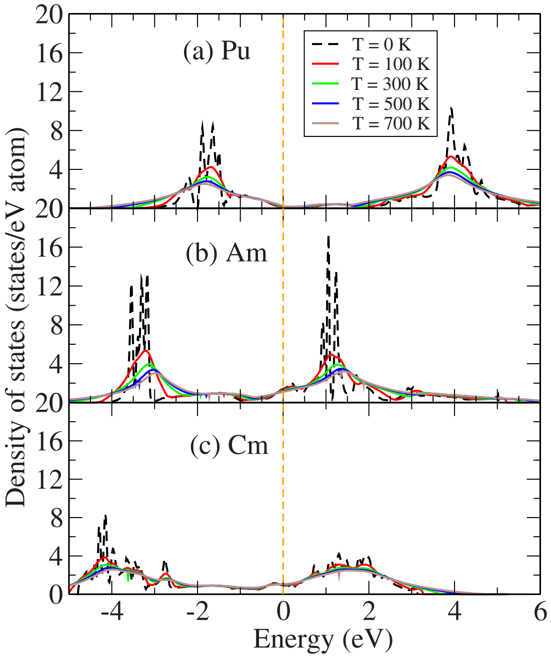

FIG. 5. (Color online) Temperature dependence of DOS in Pu, Am, and Cm.

since strong electron-impurity interaction can significantly correct this result. In this paper, only the "phonon" part of total ER in Cm was found. The obtained ER is a linear function of temperature with positive TCR in the interval of 100–350 K, and has a behavior similar to that of Pu and Am at higher temperature. That is why the DOS value in Cm at the Fermi level is kept unchanged with temperature and only the T/Θ factor determines ER temperature behavior. Note that from 500 to 700 K, and up to its high temperature limit, the ER of metals demonstrates weak temperature dependence due to strong erosion of DOS at the Fermi level.

The ER calculations for pure fcc Pu, Am, and Cm at high temperatures predict typical metallic behavior of ER over the whole temperature region, without any specific peculiarities. The obtained ER demonstrates a similar behavior with temperature without any anomalies compared with ER data in the other 4-(5-)*d* transition and 4-(5-)*f* rare-earth metals.

The low-temperature ER measurements[7] of 99.9% Am demonstrated $\rho \sim T^4$. This fact calls for some discussions about the physical nature of this nontypical low-temperature behavior of ER of transition metals, which is usually $\rho \sim T^5$. However, $\rho \sim T^4$ is an ordinary fact, found earlier experimentally in many nonmagnetic 3*d*-5*d* transition metals. Actually, $\rho \sim T^3 - T^4$ regularity was observed if the host *d* metal contained a number of impurities. The $\rho \sim T^5$ regularity was predicted within two-band Mott conductivity model[54] and found then experimentally for all pure nonmagnetic transition metals. So, it seems reasonable to expect $\rho \sim T^5$ behavior in pure Am. Moreover, this type of dependence was reported in early work (for more details see discussion in Ref. 7). Thus the observation of different types of ER low-temperature dependence, both $\rho \sim T^{2.8}$ and $\rho \sim T^5$ in Am, gives an additional argument in favor of our results.

In curium, observed $\rho \sim T^2$ regularity is also an ordinary fact for a metallic system which undergoes magnetic ordering.

Therefore, the analysis of calculated and experimental data allows one to conclude that all these metals are typical members of the transition metal family and that the obtained unusual ER behavior is a consequence of ordinary and well-known phenomena.

VI. CONCLUSION

Starting from the results of *ab initio* LDA+U+SO method for DOS of fcc plutonium, americium, and curium, the ER behavior of these metals and some Pu-based alloys was analyzed from the most general point of view. Mott conductivity model without any assumptions concerning the weakness of intensity of the interaction was applied to describe the ER behavior in both high- and low-temperature intervals. The negative TCR, observed experimentally in some Pu-based dilute alloys, and quadratic temperature dependence of ER at low temperatures were reproduced. Also, the "normal" metallic type of ER temperature dependence in curium and americium at high temperature and $\rho \sim T^2$ and $\rho \sim T^4$ regularities at low temperature, respectively, was explained.

It was demonstrated that the interference of different types of scattering (electron-phonon and electron-impurity) has to correlate with the renormalization of a ground state energy in Pu-based alloys and leads to negative TCR. Hence, in these alloys, a new local minimum is formed in the total energy curve that might be relevant to the understanding of stability of Pu-based alloys.

Since the DOS values at the Fermi level in *d* and *f* bands are almost the same, the scattering of *s* electron into *d* and *f* bands has the same probability. Therefore, mobile *s*-type electrons are able to fill up the empty *d* and *f* states due to such scattering, and thus, can cause the weak magnetic moments observed in some Pu-based alloys.[15,29] The correlation between the above-mentioned specific electron scattering and magnetic properties is of interest in further investigations.

ACKNOWLEDGMENTS

This research was supported by programs "Nanoheterostructures" (SS 5869.2006.2) and the Russian Foundation for Basic Research (Projects Nos. 06-02-81017 and 07-02-00041). M.A.K. acknowledges support of Russian Science Support Foundation. A.V.L. and M.A.S. acknowledge support from the Dynasty Foundation and International Centre for Fundamental Physics.

---

*y.tsiovkin@imp.uran.ru

[1] R. Smoluchowskii, Phys. Rev. **125**, 1577 (1962).

[2] M. B. Brodsky, Phys. Rev. **137**, A1423 (1965).

[3] A. R. Harvey, M. B. Brodsky, and W. J. Nellis, Phys. Rev. **139**, A437 (1965).

[4] S. Hecker, Los Alamos Sci. **26**, 16 (2000).

[5] A. M. Boring and J. L. Smith, Los Alamos Sci. **26**, 90 (2000).

[6] P. Boulet, F. Wastin, E. Coliheau, J. C. Griveau, and J. Rebizant, J. Phys.: Condens. Matter **15**, S2305 (2003).

[7] W. Muller, R. Schenkel, H. E. Schmidt, J. C. Spirlet, D. L. McElroy, R. O. A. Hall, and M. J. Mortimer, J. Low Temp. Phys. **30**, 561 (1978).

[8] N. Baclet, M. Dormeval, L. Havela, J. M. Fournier, C. Valot, F. Wastin, T. Gouder, E. Colineau, C. T. Walker, S. Bremier, C. Apostolidis, and G. H. Lander, Phys. Rev. B **75**, 035101 (2007).

[9] R. Schencel, Solid State Commun. **23**, 389 (1977).

[10] M. B. Brodsky, Rep. Prog. Phys. **41**, 1547 (1978).

[11] A. J. Arco, M. B. Brodsky, and W. J. Nellis, Phys. Rev. B **5**, 4564 (1972).

[12] V. Dallacasa, J. Phys. F: Met. Phys. **11**, 177 (1981).

[13] S. Méot-Reymond and J. M. Fournirer, J. Alloys Compd. **232**, 119 (1996).

[14] R. Jullien, M. T. Beal-Monod, and B. Cogblin, Phys. Rev. B **9**, 1441 (1974).

[15] M. Fluss, B. D. Wirth, M. Wall, T. E. Felter, M. J. Caturla, A. Kubota, and T. Diaz de la Rubia, J. Alloys Compd. **368**, 62

(2004).
[16] T. Aisaka and M. Shimizu, J. Phys. Soc. Jpn. **28**, 646 (1970); J. Jhod and M. Shimizu, *ibid.* **41**, 1211 (1972).
[17] Yu. Piskunov, K. Mikhalev, A. Gerashenko, A. Pogudin, V. Ogloblichev, S. Verkhovskii, A. Tankeyev, V. Arkhipov, Yu. Zouev, and S. Lekomtsev, Phys. Rev. B **71**, 174410 (2005).
[18] S. V. Verkhovskii, V. E. Arkhipov, Yu. N. Zuev, Yu. V. Piskunov, K. N. Mikhalev, A. V. Korolev, I. L. Svyatov, A. V. Pogudin, V. V. Ogloblichev, and A. L. Buzlukov, JETP Lett. **82**, 139 (2005).
[19] J. C. Lashley, J. Singleton, A. Migliori, J. B. Betts, R. A. Fisher, J. L. Smith, and R. J. McQueeney, Phys. Rev. Lett. **91**, 205901 (2003).
[20] P. G. Huray, S. E. Nave, J. R. Peterson, and R. G. Haire, Physica B & C **102**, 217 (1980).
[21] Yu. Yu. Tsiovkin and L. Yu. Tsiovkina, J. Phys.: Condens. Matter **19**, 056207 (2007).
[22] W. Kohn and L. J. Sham, Phys. Rev. **140**, A1133 (1965).
[23] A. O. Shorikov, A. V. Lukoyanov, M. A. Korotin, and V. I. Anisimov, Phys. Rev. B **72**, 024458 (2005).
[24] P. Söderlind and B. Sadigh, Phys. Rev. Lett. **92**, 185702 (2004).
[25] A. B. Shick, V. Drchal, and L. Hevela, Europhys. Lett. **69**, 588 (2005).
[26] K. T. Moore, G. van der Laan, R. G. Haire, M. A. Wall, A. J. Schwartz, and P. Söderlind, Phys. Rev. Lett. **98**, 236402 (2007).
[27] A. Landa, P. Söderlind, and A. Ruban, J. Phys.: Condens. Matter **15**, L371 (2003).
[28] V. I. Anisimov, A. O. Shorikov, and J. Kuneš, doi:10.1016/j.jallcom.2006.10.150.
[29] S. McCall, M. J. Fluss, B. W. Chung, G. F. Chapline, D. D. Jackson, and M. W. McElfresh, *Emerging Magnetism Arising from Self Damage in* α *and* δ*-Pu*, MRS Symposia Proceedings No. 893 (Materials Research Society, Pittsburgh, 2006), p. 0893-JJ04-03.1.
[30] S. Yu. Savrasov and G. Kotliar, Phys. Rev. Lett. **84**, 3670 (2000).
[31] S. Yu. Savrasov, G. Kotliar, and E. Abrahams, Nature (London) **410**, 793 (2001).
[32] J. C. Lashley, A. Lawson, R. J. McQueeney, and G. H. Lander, Phys. Rev. B **72**, 054416 (2005).
[33] R. H. Heffner, G. D. Morris, M. J. Fluss, B. Chung, D. E. MacLaughlin, L. Shu, and J. E. Anderson, Physica B **374-375**, 163 (2006).
[34] J. H. Shim, K. Haule, and G. Kotliar, Nature (London) **446**, 513 (2007).
[35] A. Shick, J. Kolorenc, L. Havela, V. Drchal, and Th. Gouder, Europhys. Lett. **77**, 17003 (2007).
[36] S. Y. Savrasov, K. Haule, and G. Kotliar, Phys. Rev. Lett. **96**, 036404 (2006).
[37] L. V. Pourovskii, G. Kotliar, M. I. Katsnelson, and A. I. Lichtenstein, Phys. Rev. B **75**, 235107 (2007).
[38] M. B. Brodsky, Phys. Rev. B **9**, 1381 (1974).
[39] J. H. Mooij, Phys. Status Solidi A **17**, 521 (1973).
[40] X. Dai, S. Yu. Savrasov, G. Kotliar, A. Miglior, H. Ledbetter, and E. Abrahams, Science **300**, 953 (2003).
[41] N. F. Mott, Adv. Phys. **13**, 325 (1964).
[42] Yu. Yu. Tsiovkin and A. N. Voloshinskii, Fiz. Met. Metallogr. **75**, 229 (1993).
[43] A. Lindbaum, S. Heathman, K. Litfin, Y. Méresse, R. G. Haire, T. Le Bihan, and H. Libotte, Phys. Rev. B **63**, 214101 (2001).
[44] S. Heathman, R. G. Haire, T. Le Bihan, A. Lindbaum, M. Idiri, P. Normile, S. Li, R. Ahuja, B. Johansson, and G. H. Lander, Science **309**, 110 (2005).
[45] W. E. Pickett, S. C. Erwin, and E. C. Ethridge, Phys. Rev. B **58**, 1201 (1998).
[46] A. N. Voloshinskii and A. G. Obukhov, Phys. Met. Metallogr. **91**, 238 (2001).
[47] A. B. Chen, G. Weisz, and A. Sher, Phys. Rev. B **5**, 2897 (1972).
[48] *The Actinides*, edited by A. J. Freeman and G. H. Lander, Handbook of Physics and Chemistry Vol. 5 (Elsevier Science, New York, 1987).
[49] W. A. Harrison, Phys. Rev. B **64**, 235112 (2001); *Electronic Structure and Properties of Solids* (Freeman, San Francisco, 1980).
[50] M. J. Graf, T. Lookman, J. M. Wills, D. C. Wallace, and J. C. Lashley, Phys. Rev. B **72**, 045135 (2005).
[51] Yu. Yu. Tsiovkin, A. N. Voloshinskii, V. V. Gapontsev, V. V. Ustinov, A. G. Obykhov, A. L. Nikolaev, I. A. Nekrasov, and A. V. Lukoyanov, Phys. Rev. B **72**, 224204 (2005).
[52] S. I. Abramenko, E. E. Zakurdaev, A. M. Lyasota, and A. V. Troshev, Proceedings of the VII International Ural Seminar on Radiation Damage Physics of Metals and Alloys, p. 55, Snezhinsk, Russia, February 2007 (unpublished).
[53] Yu. M. Kagan and A. P. Zernov, Sov. Phys. JETP **50**, 1107 (1966).
[54] N. G. Shelushinina and A. N. Voloshinskii, Fiz. Met. Metallogr. **32**, 925 (1971); **32**, 1147 (1971).